Digest Journal of Nanomaterials and Biostructures Vol. 14, No. 1, January - March 2019, p. 153 - 159

APPLICATION OF ZnO SCHOTTKY DIODES IN RECTIFIER CIRCUITS FOR IMPLEMENTATION IN ENERGY HARVESTING

M. GOMEZ-ALVAREZ[a*], I. MEJIA[b], V. CABRERA[a], C. AVILA-AVENDANO[b], R. GARCÍA[c], A. DIAZ-CANO[a], Y. LEON-NATARET[a], M. QUEVEDO-LOPEZ[b], L. RESÉNDIZ[a]

[a]*Instituto Politécnico Nacional, Section of Postgraduate Studies and Research, Mexico City, 07340, Mexico*
[b]*Department of Materials Science and Engineering, The University of Texas at Dallas, Richardson 75080, TX, USA*
[c]*Ecatepec University Center, Autonomous Mexico State University, Ecatepec (UAEMex), 55020, Mexico*

This work presents the results obtained from the SPICE simulation of a full-wave bridge rectifier circuit, a double half-wave rectifier circuit and a half-wave rectifier circuit, each at a frequency of 816MHz and low amplitude. The results match the experimental I–V curves obtained with the parameters extracted from the electrical characteristics of the experimental Schottky diodes: Si/SiO_2/Cr/Au/ZnO/Al, glass/Al/ZnO/Au and glass/Al/ZnO/Pd. The results of the simulation show that the devices fabricated in this work can be a useful alternatives for rectifier circuits commonly used in energy harvesting systems, because they are capable of delivering output rectified voltages higher than 1V.

(Received September 19, 2018; Accepted February 21, 2019)

Keywords: Energy harvesting, Rectifiers, Schottky diodes

1. Introduction

Portable applications using power from energy harvesters systems consume very low levels of power. Therefore, the corresponding AC-DC power converter stage in energy harvesters needs to operate with ultra-low-voltage input. For low-power electronics requiring an input of only a few milliwatts, harvesting energy from the environment has become feasible [1], [2]. The energy harvester is configured of a dipole antenna, which captures and stores the environmental energy (external sources); a balun, which is responsible for transforming a balanced system (dipole antenna) into an unbalanced system (matching network and the rectifier circuit) to be connected to each other. The matching network is responsible for impedance coupling for the proper termination of the current, and the rectifier circuit can convert the AC input voltage into DC output voltage [3].

Moreover, recent developments in thin film electronics and thin film sensors have driven the implementation of thin film energy harvesters as well. In 2013, the first UHF energy harvester was fabricated using Schottky diodes of indium-gallium-zinc oxide IGZO, enabling it to deliver 1.3 V at a radius of 15 cm from the source antenna, which emits 15dBm to 868 MHz [4]. Diodes and rectifier circuits have been demonstrated to perform at high-frequency (HF) operation (~ MHz) of diodes and circuits rectifier circuits using organic semimetals as active layers [5], [6], [7], [8], [9].

This work uses preliminary data from the electrical characteristics of ZnO Schottky diodes. The electrical device parameters were extracted, and simulations were performed at frequency of 816 MHz at 3 V for a double half wave rectifier circuit, a full-wave bridge rectifier circuit and a half wave rectifier circuit. Simulations showed these circuits to be capable of

* Corresponding author: mgomeza1700@alumno.ipn.mx

delivering more than 1 V output to a resistive load, which can be connected to a matching network in energy harvesting systems.

2. Experimental details

Three configurations of vertical devices were fabricated using 10/120 nm of Cr/Au and 190 nm of Al electrodes were deposited by e-beam evaporation on Si and glass substrates, respectively. Afterwards a 73 nm-thick of ZnO layer was deposited using RF sputtering. The optimized deposition parameters used during deposition of ZnO thin films are shown in Table 1. The deposited ZnO thin films were exposed to a fast thermal annealing at 200ºC for 30 min in an air environment. As the final step, Al, Au and Pd top contacts were deposited by e-beam evaporation through a molybdenum shadow mask. The final structures of the Schottky diodes were Si/SiO_2/Cr/Au/ZnO/Al, glass/Al/ZnO/Au and glass/Al/ZnO/Pd. The crystal structure of the ZnO thin films was analyzed by X-ray diffraction (XRD) (Rigaku Ultima III, Cu-Kα=0.1542 nm). Current-voltage (I–V) measurements were carried out with the parameters analyzer (Keithley 4200). SPICE simulations of a full-wave bridge rectifier, a double half-wave rectifier, and a half-wave rectifier, were performed using the parameters extracted from the I–V measurements of Schottky diodes.

Table 1. Deposition parameter.

Target to substrate distance (cm)	12.5
Vacuum pressure (Torr)	3.9×10^{-6}
Deposition pressure (Torr)	4.0×10^{-3}
RF power (W)	51
Argon gas concentration (sccm)	12
Deposition time (min)	60

3. Results and discussion

The XRD pattern of the ZnO/Al thin films deposited on the glass substrate is shown in Fig. 1. In the XRD spectra, the broad and intense diffraction (0 0 2) peak (2θ = 34.42°) indicates that the ZnO thin films had a wurtzite hexagonal structure and were well-oriented on the C-axis, meaning that the ZnO thin films had a suitable adhesion to the Al/glass substrate [10]. The diffraction peaks corresponding to (1 0 1) and (1 0 2) ZnO with very low intensity, indicating poor crystalline orientation, were also observed. The peak at 38.46° and 44.69° can be attributed to Al(1 1 1) and Al(2 0 0) deposited on the glass substrate, respectively [11].

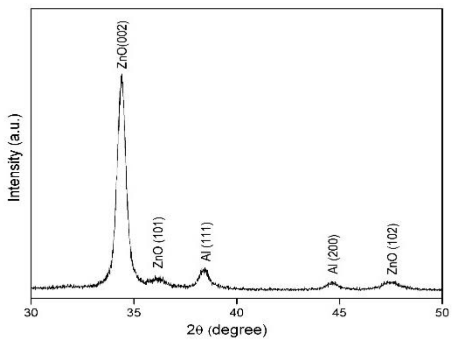

Fig. 1. XRD of ZnO/Al deposited on glass.

Room temperature (293 K) I–V characteristics of Schottky diodes with different structures were measured, the results of which are shown in Fig. 2 (a). The highest rectification ratio (I_F/I_R) at ± 1.5 V of 2.3×10^5 was achieved by Si/SiO_2/Cr/Au/ZnO/Al, followed by glass/Al/ZnO/Au with 1081, and glass/Al/ZnO/Pd with 222. The threshold voltage of each Schottky diode was less than 0.4 V. The I–V characteristics of the Schottky diode were analyzed using conventional thermionic emission theory. The I–V relation is given by Rajan, Periasamy and Shauli [12]

$$I = I_s[\exp(qV - IR_s/nkT) - 1] \tag{1}$$

where I_s is the reverse saturation current, given by Avdogan et al. [13]

$$I_s = AR^*T^2 \exp(-q\Phi_b/kT) \tag{2}$$

in which q is the electron charge, and R^* is the effective Richardson constant, which, has a theoretical value of 32 A/cm^2K^2 for ZnO. A is the effective area of the diode. T is the temperature in Kelvin, k is Boltzmann's constant, Φ_b is the barrier height, and V is the applied voltage.

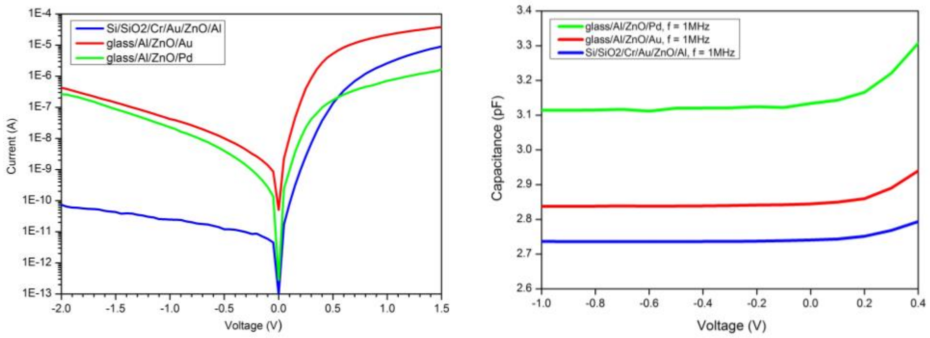

a) *b)*

Fig. 2. Electrical characteristics of Schottky diodes (a) I–V measurements and (b) C–V measurements at reverse bias voltage.

I_s is derived from the straight-line intercept of Ln*(I)* at *V*=0. The ideality factor n can be determined from the slope of the linear region of the forward bias Ln*(I)–V* curve by

$$n = q/kT\,(dV/d\ln I) \tag{3}$$

Values of $I_s$were used to calculated Φ_b by

$$\Phi_b = kT\ln(AR^*T^2/I_s) \tag{4}$$

The series resistance R_s can be determined from the value of the slope of forward bias $VR_s - I$ by

$$IR_s = V - (n\,kT/q)\ln(I/I_s) = VR_s \tag{5}$$

The capacitance of a Schottky junction is given by

$$A^2/C^2 = (2/\varepsilon_S\varepsilon_0 N_d)(\Phi_{bi} - kT/q - V) \tag{6}$$

where ε_S is the static dielectric constant of the semiconductor, which, has a value of 10.8, ε_0 is the dielectric constant of a vacuum, N_d is the donor carrier concentration and Φ_{bi} is the built-in potential [14]. Fig. 2(b) shows the C–V characteristics of the Schottky diodes at a reverse bias. The devices`s small area of 200 µm reduces the capacitance considerably to values less than 3.2 pF at reverse bias. The low values of capacitance, in turn, enable a high operational frequency. The electrical characteristics of the diodes extracted from the I–V and C–V measurements are shown in Table 2.

Table 2. Characteristics of Schottky diodes extracted from I–V measurements.

	$Si/SiO_2/Cr/Au/ZnO/Al$	glass/Al/ZnO/Au	glass/Al/ZnO/Pd
ideality factor n	1.5	1.5	1.6
barrier height Φ_b (eV)	0.78	0.61	0.64
saturation current I_s (A)	6.1×10^{-12}	8.1×10^{-10}	3.9×10^{-10}
series resistance R_s (KΩ)	50.746	27.496	101.438
capacitance at 0V C_{j0} (pF)	2.73	2.84	3.12

The simulations I–V characteristics of the ZnO Schottky diodes are showed in Fig. 3(a)-(c). It is evident that the values of the parameters in Table 2 achieve an agreement in fitting between the experimental data and the simulations.

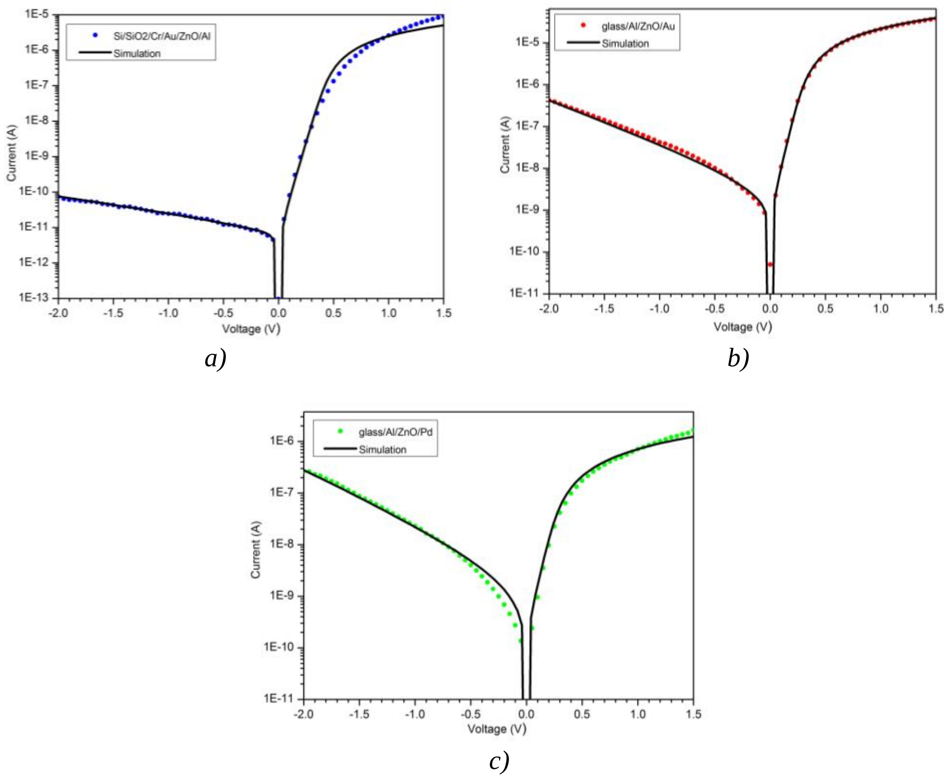

Fig. 3. Simulated and experimental I–V characteristics of Schottky diodes (a) glass/Al/ZnO/Pd, (b) Si/SiO_2/Cr/Au/ZnO/Al and (c) glass/Al/ZnO/Au.

Circuits schematics of the full-wave bridge rectifier, of the double half-wave rectifier, and of the half-wave rectifier are shown in the Fig. 4(a)-(c), respectively. In the double half-wave rectifier, to rectify half of the AC input, voltage D_1 is on and charges the capacitance positively, while for the other half of the input voltage D_2 charges the capacitance negatively.

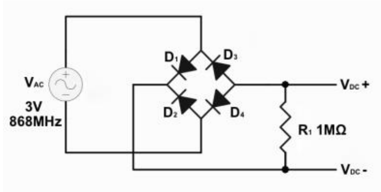

a)

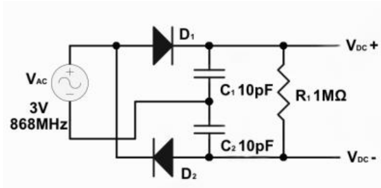

b)

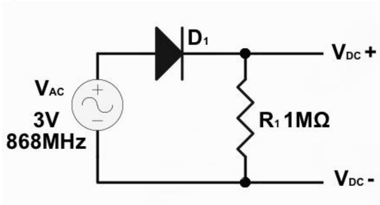

c)

Fig. 4. Circuits schematics of rectifiers (a) a full-wave bridge, (b) a double half-wave and (c) a half-wave.

Fig. 5(b) shows the simulations of the double half-wave rectifier with is maximum rectified voltage V_{OUT} as a function of the AC input signal frequency with an amplitude of 2 V and with a resistive load at the output of 1MΩ. These simulations were carried out using the parameters described in Table 2 for the Schottky diodes with structure glass/Al/ZnO/Au, because of their higher values of forward bias current. In Fig. 5(b), at low frequencies the maximum rectified voltage is equal to 0.98 V due to the ~0.4 V threshold voltage of fabricated Schottky diodes. At higher frequencies, the output voltage decreases significantly, achieving in a maximum signal cutoff frequency of 816 MHz.

Using the extracted parameters shown in Table 2, the authors carried out simulations of rectified output voltage V_{OUT} as a function of the time. These results of the simulations of a full-wave bridge rectifier circuit, a double half-wave rectifier, and a half-wave rectifier are shown in Fig. 5(a)-(c), respectively. The simulations were carried out using the cutoff frequencies of the fabricated diodes, which are also typical characteristics of the energy harvester, ultra-high frequency (UHF=816 MHz) and low amplitude (3 V). Although the Schottky diodes with structure Si/SiO_2/Cr/Au/ZnO/Al exhibited a higher barrier height Φ_b=0.78 eV, the Schottky diodes with structure glass/Al/ZnO/Au showed higher rectified maximum voltages due to their lower resistance series R_s=27.496 KΩ. 2.77, 1.41 and 1.61 V are the rectified maximum voltages of glass/Al/ZnO/Au for the full wave-bridge rectifier, double half-wave rectifier and half-wave rectifier, respectively. In addition, the Schottky diodes with structures: Si/SiO_2/Cr/Au/ZnO/Al and glass/Al/ZnO/Pd, also exhibited maximum rectified voltages higher than 1 V due to a suitable fabrication process that generated optimal electrical characteristics. The results of the simulations show that these rectifier circuits could be a viable option to be used as voltage rectifiers in portable devices, such as energy harvesters. However, to be implemented in physical applications, the diodes have to be assembled to a harvester antenna using a matching network.

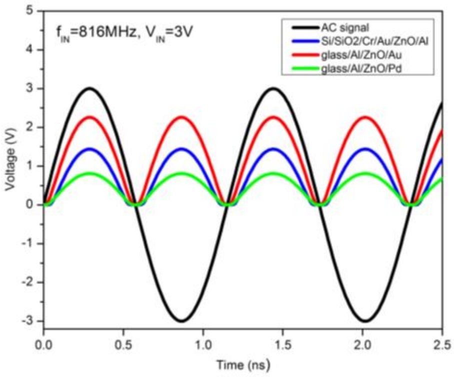

a)

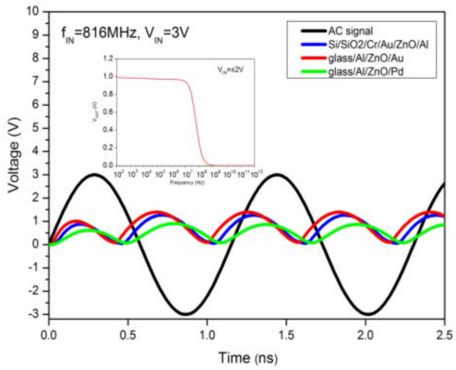

b)

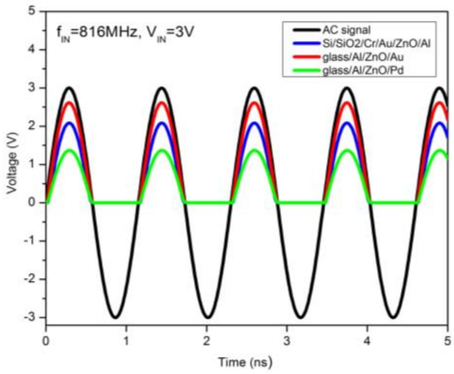

c)

Fig. 5. Simulated output voltage of the rectifier circuits of (a) a full-wave bridge, (b) a double half-wave (voltage V_{OUT} as a function of the applied AC frequency with an amplitude of 2 V for RL=1MΩ inside graph) and (c) a half-wave.

4. Conclusions

In summary, highly C-axis oriented ZnO films were deposited on the Al/glass and Schottky diodes with structures: Si/SiO_2/Cr/Au/ZnO/Al, glass/Al/ZnO/Au, and glass/Al/ZnO/Pd, were successfully fabricated. The I–V characteristics show the rectifying nature of the diodes, with an ideality factor of n=1.5, barrier height of Φ_b=0.78 eV and saturation current of $I_S = 6.1 \times 10^{-12}$ A. The I–V simulations are in agreement with the experimental data. In the simulations, the results of a full-wave bridge rectifier circuit, a double half-wave rectifier circuit, and a half-wave rectifier circuit, at 816 MHz (UHF) and 3 V amplitude (low amplitude), the devices show maximum rectified voltages greater than 1 V, which proves their possible application in energy harvesting systems.

Acknowledgements

This work was supported in part by SIP−IPN project 20181363. The work of Miguel Gomez was supported by the National Fellowship from Consejo Nacional de Ciencia y Tecnología (CONACYT).

References

[1] A. Chasin, S. Steudel, K. Myny, M. Nag, T.H. Ke, S. Schols, J. Genoe, G. Gielen, P. Heremans, Appl. Phys. Lett. **101**(113505), 1 (2012).

[2] A. Chasin, S. Steudel, F. Vanaverbeke, K. Miny, M. Nag, T.H. Ke, S. Schols, G. Gielen, J. Genoe, P. Heremans, IEDM Tech. Dig. **88**(12), 287 (2012).
[3] A. Chasin, M. Nag, A. Bhoolokman, K. Miny, S. Steudel, S. Schols, J. Genoe, G. Gielen, P. Heremans, IEEE Trans. Electron D. **60**(10), 3407 (2013).
[4] A. Chasin, V. Volskiy, M. Libois, M. Ameys, M. Nag, M. Rockele, K. Myny, S. Steudel, S. Schols, Guy A. E. Vandenbosch, W. de Raedt, J. Genoe, G. Gielen, P. Heremans, IEEE Trans. Electron Dev. **13**(11), 292 (2013).
[5] S. Steudel, K. Myny, V. Arkhipov, C. Deibel, S. Vusser, J. Genoe, P. Heremans, Nature Mater. **4**, 597 (2005).
[6] S. Steudel, S. Vusser, K. Myny, M. Lenes, J. Genoe, P. Heremans, J. Appl. Phys. **99**(114519), 1 (2006).
[7] D. Im, H. Moon, M. Shin, J. Kim, S. Yoo, Adv. Mater. **23**(5), 644 (2011).
[8] P. Heljo, K. E. Lilja, H. S. Majumdar, D. Lupo, Organic Electron. **15**, 306 (2014).
[9] C. Y. Lin , C. H. Tsai, H. T. Lin, L. C. Chan, Y. H. Yeh, Z. Pei, Y. R. Peng, C. C. Wu, Organic Electron. **12**, 1777 (2011).
[10] W. T Lim, C. H Lee, Thin Solid Films **353**, 12 (1999).
[11] G. Yuan, Z. Ye, L. Zhu, J. Huang, Q. Qian, B. Zhao, J. Cryst. Growth. **268**, 169 (2004).
[12] L. Rajan, C. Periasamy, V. Sahula, Perspectives in Science **8**, 66 (2016).
[13] S. Aydogan, K. Cinar, H. Asil, C. Coskun, A. Turut, J. Alloys Compd. **476**, 913 (2009).
[14] B. K. Patel, K. K. Nanda, S. N. Sahu, J. Appl. Phys. **85**(7), 3666 (1999).